

Symmetric Z_2 spin liquids and their neighboring phases on triangular lattice

Yuan-Ming Lu¹

¹*Department of Physics, The Ohio State University, Columbus, OH 43210, USA*

Motivated by recent numerical discovery of a gapped spin liquid phase in spin-1/2 triangular-lattice J_1 - J_2 Heisenberg model, we classify symmetric Z_2 spin liquids on triangular lattice in the Abrikosov-fermion representation. We find 20 phases with distinct spinon symmetry quantum numbers, 8 of which have their counterparts in the Schwinger-boson representation. Among them we identify 2 promising candidates (#1 and #20), which can realize a gapped Z_2 spin liquid with up to next nearest neighbor mean-field amplitudes. We analyze their neighboring magnetic orders and valence bond solid patterns, and find one state (#20) that is connected to 120-degree Neel order by a continuous quantum phase transition. We also identify gapped nematic Z_2 spin liquids in the neighborhood of the symmetric states and find 3 promising candidates (#1, #6 and #20).

PACS numbers: 71.27.+a, 75.10.Kt

I. INTRODUCTION

Thanks to advances in numerical methods and increasing computational power, recently a lot of progress has been made in the pursuit of quantum spin liquids^{1,2} (QSLs) in various frustrated quantum spin models³⁻¹³. In contrast to classical paramagnets driven by thermal fluctuations, QSLs are symmetric zero-temperature phases featured by collective excitations which obey fractional statistics¹⁴⁻¹⁶ and long-range quantum entanglement^{17,18} therein. Most recently using the density matrix renormalization group (DMRG) method, two numerical studies^{12,13} of the spin-1/2 Heisenberg J_1 - J_2 model on triangular lattice independently reported strong evidence for a gapped spin liquid phase^{12,13} in the finite range of J_2/J_1 , sandwiched by a noncollinear 120-degree Neel order at smaller J_2/J_1 and a collinear stripy Neel order at larger J_2/J_1 . This is also supported by earlier variational Monte Carlo studies^{19,20} on the same model. Due to its similarity to the gapped Z_2 spin liquid phase discovered in kagome Heisenberg model^{3,5,6}, this discovery motivates us to look for symmetric Z_2 spin liquid phases on triangular lattice as possible candidates for the one realized in J_1 - J_2 model.

A symmetric Z_2 spin liquid hosts 3 types of fractionalized excitations: bosonic spinon b , bosonic vison v and fermionic spinon f . Each of them obeys mutual semionic statistics¹⁶ with the other two. Unlike usual ordered phases characterized by their broken symmetries, symmetric spin liquids are characterized by the symmetry quantum numbers of their fractional excitations. In particular, each quasiparticle can carry a fraction of the unit symmetry quantum number carried by a fundamental particle (such as a magnon in frustrated magnets), these phenomena are generally coined “symmetry fractionalization”^{21,22}. Take Z_2 spin liquids for instance, each spinon carries spin-1/2, half of the spin quantum number carried by each magnon. Taken into account of time reversal, spin rotation and space group symmetries,

there are many different symmetric Z_2 spin liquids with distinct quasiparticle symmetry quantum numbers. Instead of attempting to fully classify²¹⁻²³ all possible Z_2 spin liquids on triangular lattice, in this work we restrict ourselves to the Abrikosov-fermion representation²⁴⁻²⁶, which is a convenient way to construct variational wavefunctions of Z_2 spin liquids. Among 20 distinct symmetric states in Abrikosov-fermion representation, we identify two promising candidates (#1 and #20 in TABLE I) that can realize a gapped Z_2 spin liquid with up to next nearest neighbor mean-field amplitudes.

Since the gapped spin liquid appears in proximity to two magnetic orders in DMRG studies^{12,13}, it’s desirable to understand the symmetry-breaking phases in the neighborhood of symmetric Z_2 spin liquids. In particular, a Z_2 spin liquid can enter either a noncollinear magnetic order^{27,28} or a valence bond solid (VBS) phase^{29,30} via continuous quantum phase transitions, by condensing either bosonic spinons b or visons v . In this work, we study the magnetic and VBS phases in the neighborhood of the two gapped Z_2 spin liquids, #1 and #20 in TABLE I. In particular we find that #20 can be driven into 120-degree noncollinear Neel order by a continuous quantum phase transition.

In DMRG studies of triangular J_1 - J_2 model, strong evidence for nematic order *i.e.* breaking of 6-fold rotational symmetry has been observed^{12,13}. In this work we also explore the possibility of gapped nematic spin liquids in the neighborhood of symmetric spin liquids. In addition to the 2 symmetric candidates (#1 and #20), we identify another promising nematic gapped state *i.e.* #6 in TABLE I. The mean-field ansatz of #6 and #20 nematic states are depicted in FIG. 3 and 2.

This paper is organized as follows. In section II we classify 20 distinct symmetric Z_2 spin liquids in the Abrikosov-fermion representation, as summarized in TABLE I. We also unify the 8 previously obtained Z_2 spin liquids in the Schwinger-boson representation³¹ with our Abrikosov-fermion states. In section III we propose 2

promising candidates (#1 and #20 in TABLE I) among all 20 symmetric states for the J_1 - J_2 spin liquid phase, and study the magnetic orders and VBS patterns in the neighborhood of these 2 promising candidates. In section IV we introduce nematic order into symmetric states, to achieve nematic Z_2 spin liquids on triangular lattice. We find 3 promising gapped nematic Z_2 spin liquids (#1, #6 and #20 in TABLE I, see FIG. 2 and 3) that may be realized in triangular-lattice J_1 - J_2 model. Finally concluding remarks are given in section V.

II. CLASSIFYING SYMMETRIC Z_2 SPIN LIQUIDS ON TRIANGULAR LATTICE

We label each lattice site on a triangular lattice by its positional vector $\mathbf{r} = x\vec{a}_1 + y\vec{a}_2 \equiv (x, y)$, where $\vec{a}_1 = a(1, 0)$ and $\vec{a}_2 = a(-1, \sqrt{3})/2$ are chosen to be two Bravais vectors as shown in FIG. 1. The crystal symmetry group is generated by two translations $T_{1,2}$, mirror reflection σ and site-centered $\pi/3$ rotation C_6

$$\begin{aligned} (x, y) &\xrightarrow{T_1} (x+1, y), & (x, y) &\xrightarrow{T_2} (x, y+1), \\ (x, y) &\xrightarrow{\sigma} (y, x), & (x, y) &\xrightarrow{C_6} (x-y, x). \end{aligned} \quad (1)$$

These crystal symmetries, together with global time reversal \mathbf{T} and $SU(2)$ spin rotational symmetries impose constraints on a gapped Z_2 spin liquids. These symmetry conditions give rise to distinct Z_2 spin liquids in the Abrikosov-fermion representation.

A. Classifying Z_2 spin liquids in Abrikosov-fermion representation

In Abrikosov-fermion representation^{24,25}, a spin 1/2 on lattice site \mathbf{r} is written in terms of two fermions $f_{\mathbf{r},\uparrow/\downarrow}$:

$$\vec{S}_{\mathbf{r}} = \frac{1}{4} \text{Tr}(\Psi_{\mathbf{r}}^\dagger \Psi_{\mathbf{r}} \vec{\sigma}), \quad \Psi_{\mathbf{r}} \equiv \begin{pmatrix} f_{\mathbf{r},\uparrow} & f_{\mathbf{r},\downarrow} \\ f_{\mathbf{r},\downarrow}^\dagger & -f_{\mathbf{r},\uparrow}^\dagger \end{pmatrix} \quad (2)$$

where $\vec{\sigma}$ stands for Pauli matrices. First we construct mean-field Hamiltonian (“ansatz”) for fermionic spinons

$$H_{MF} = \sum_{\mathbf{r},\mathbf{l}} \text{Tr}(\Psi_{\mathbf{r}}^\dagger \langle \mathbf{r}|\mathbf{l} \rangle \Psi_{\mathbf{l}}), \quad \langle \mathbf{r}|\mathbf{l} \rangle = \langle \mathbf{l}|\mathbf{r} \rangle^\dagger. \quad (3)$$

where mean-field amplitudes $\langle \mathbf{r}|\mathbf{l} \rangle$ preserve all symmetries. Then the many-spin wavefunction can be obtained by Gutzwiller projection which enforces the following single-occupancy constraint

$$f_{\mathbf{r},\uparrow}^\dagger f_{\mathbf{r},\uparrow} + f_{\mathbf{r},\downarrow}^\dagger f_{\mathbf{r},\downarrow} = 1 \quad (4)$$

on the mean-field groundstate $|MF\rangle$ of fermionic spinons. There is a $SU(2)$ gauge redundancy^{25,26,32} in this representation: spin operators $\vec{S}_{\mathbf{r}}$ remains invariant under local $SU(2)$ gauge rotation $\Psi_{\mathbf{r}} \rightarrow W_{\mathbf{r}} \Psi_{\mathbf{r}}$, $W_{\mathbf{r}} \in SU(2)$.

Therefore each physical symmetry operation \hat{u} is followed by a $SU(2)$ gauge rotation $G_{\hat{u}}(\mathbf{r})$ when acting on fermionic spinons. It follows that distinct Z_2 spin liquids are classified by so-called *projective symmetry group* (PSG)²⁶: *i.e.* gauge-inequivalent symmetry operations $\{G_{\hat{u}}(\mathbf{r})|\hat{u} \in \text{symmetry group}\}$ with $G_{\mathbf{e}}(\mathbf{r}) = \pm 1 \in Z_2$ for the identity element \mathbf{e} of symmetry group.

In our case of triangular lattice, the symmetry group (including spin rotations, time reversal \mathbf{T} and space group generated by $T_{1,2}, \sigma, C_6$) imposes the algebraic conditions summarized on the left column of TABLE II for symmetry operations $\{G_{\hat{u}}(\mathbf{r}) \in SU(2)\}$. The gauge-inequivalent solutions are the following:

$$\begin{aligned} G_{T_1}(x, y) &= 1, & G_{T_2}(x, y) &= \eta_{12}^x, \\ G_{\sigma}(x, y) &= \eta_{12}^{xy} g_{\sigma}, & G_{C_6}(x, y) &= \eta_{12}^{xy+y(y-1)/2} g_{C_6}, \\ G_{\mathbf{T}}(x, y) &= g_{\mathbf{T}}. \end{aligned} \quad (5)$$

with

$$\begin{aligned} g_{\sigma}^2 &= \eta_{\sigma}, & g_{C_6}^6 &= \eta_{C_6}, & (g_{C_6} g_{\sigma})^2 &= \eta_{\sigma C_6}, \\ g_{\mathbf{T}}^2 &= \eta_{\mathbf{T}}, & g_{\sigma} g_{\mathbf{T}} &= g_{\mathbf{T}} g_{\sigma} \eta_{\sigma \mathbf{T}}, & g_{C_6} g_{\mathbf{T}} &= g_{\mathbf{T}} g_{C_6} \eta_{C_6 \mathbf{T}}. \end{aligned} \quad (6)$$

Notice that we’ve defined the time reversal action $G_{\mathbf{T}}(\mathbf{r})$ on fermionic spinons $f_{\mathbf{r},\sigma}$ in the following way²⁶

$$\Phi_{\mathbf{r}} \xrightarrow{\mathbf{T}} G_{\mathbf{T}}(\mathbf{r}) \tau^2 \Phi_{\mathbf{r}} \sigma^y, \quad \Phi_{\mathbf{r}} \equiv \begin{pmatrix} f_{\mathbf{r},\uparrow} & f_{\mathbf{r},\downarrow} \\ f_{\mathbf{r},\downarrow}^\dagger & -f_{\mathbf{r},\uparrow}^\dagger \end{pmatrix}.$$

In this notation, the mean-field amplitude $\langle \mathbf{r}_1|\mathbf{r}_2 \rangle$ transforms as

$$\langle \mathbf{r}_1|\mathbf{r}_2 \rangle = -G_{\mathbf{T}}(\mathbf{r}_1) \langle \mathbf{r}_1|\mathbf{r}_2 \rangle G_{\mathbf{T}}^\dagger(\mathbf{r}_2). \quad (7)$$

under anti-unitary time reversal \mathbf{T} and

$$\langle g\mathbf{r}_1|g\mathbf{r}_2 \rangle = G_g(g\mathbf{r}_1) \langle \mathbf{r}_1|\mathbf{r}_2 \rangle G_g^\dagger(g\mathbf{r}_2). \quad (8)$$

under any (global and spatial) unitary symmetry g .

If $\eta_{\mathbf{T}} = 1$ we have $g_{\mathbf{T}} = 1$, and hence all mean-field amplitudes must vanish identically due to time reversal symmetry (7). Therefore the only physical choice is $\eta_{\mathbf{T}} = -1$ and we can choose a gauge so that $g_{\mathbf{T}} = i\tau^2 = G_{\mathbf{T}}(x, y)$, which only allows real hopping (τ^3) and real pairing (τ^1) amplitudes. With this we summarize all symmetric PSGs in TABLE I. They correspond to 20 distinct symmetric Z_2 spin liquids on triangular lattice.

Once the symmetry transformations of fermionic spinons are determined, the associated mean-field amplitudes $[x, y] \equiv \langle 0, 0|x, y \rangle$ must obey certain symmetry constraints. For example, on-site chemical potential $\hat{\mu} \equiv [0, 0]$ must satisfy

$$\begin{aligned} g_{\mathbf{T}} \hat{\mu} g_{\mathbf{T}}^\dagger &= -\hat{\mu}, \\ \hat{\mu} &= g_{\sigma} \hat{\mu} g_{\sigma}^\dagger = g_{C_6} \hat{\mu} g_{C_6}^\dagger. \end{aligned} \quad (9)$$

Symmetric Abrikosov-fermion states							Nematic states: mean-field amplitudes				Schwinger-boson states
Label	η_{12}	g_{σ}	g_{C_6}	onsite [0, 0]	NN [1, 1]	NNN [2, 1]	NN [1, 0]	NN [1, 1]	NNN [2, 1]	NNN [1, -1]	(p_1, p_2, p_3)
#1	1	τ^0	τ^0	$\tau^{1,3}$	$\tau^{1,3}$	$\tau^{1,3}$	$\tau^{1,3}$	$\tau^{1,3}$	$\tau^{1,3}$	$\tau^{1,3}$	(1,1,0)
#2	-1	τ^0	τ^0	$\tau^{1,3}$	0	0	0	0	0	0	(0,1,0)
#3	1	τ^0	$i\tau^2$	0	0	0	0	0	0	0	
#4	-1	τ^0	$i\tau^2$	0	0	$\tau^{1,3}$	$\tau^{1,3}$	0	$\tau^{1,3}$	$\tau^{1,3}$	
#5	1	τ^0	$i\tau^3$	τ^3	τ^3	τ^3	τ^3	τ^3	τ^3	τ^3	(1,1,1)
#6	-1	τ^0	$i\tau^3$	τ^3	0	τ^1	τ^1	0	τ^1	τ^1	(0,1,1)
#7	1	$i\tau^2$	τ^0	0	0	0	$\tau^{1,3}$	0	$\tau^{1,3}$	0	
#8	-1	$i\tau^2$	τ^0	0	0	0	0	0	0	0	
#9	1	$i\tau^2$	$i\tau^2$	0	0	0	0	0	0	0	
#10	-1	$i\tau^2$	$i\tau^2$	0	$\tau^{1,3}$	0	$\tau^{1,3}$	$\tau^{1,3}$	$\tau^{1,3}$	0	
#11	1	$i\tau^2$	$i\tau^3$	0	0	0	τ^3	0	τ^3	0	
#12	-1	$i\tau^2$	$i\tau^3$	0	τ^1	0	τ^1	τ^1	τ^1	0	
#13	1	$i\tau^3$	τ^0	τ^3	τ^3	τ^3	$\tau^{1,3}$	τ^3	$\tau^{1,3}$	τ^3	(1,0,0)
#14	-1	$i\tau^3$	τ^0	τ^3	0	0	0	0	0	0	(0,0,0)
#15	1	$i\tau^3$	$i\tau^1$	0	0	0	τ^1	0	τ^1	0	
#16	-1	$i\tau^3$	$i\tau^1$	0	0	τ^3	τ^3	0	τ^3	τ^3	
#17	1	$i\tau^3$	$i\tau^2$	0	0	0	0	0	0	0	
#18	-1	$i\tau^3$	$i\tau^2$	0	τ^1	τ^3	$\tau^{1,3}$	τ^1	$\tau^{1,3}$	τ^3	
#19	1	$i\tau^3$	$i\tau^3$	τ^3	τ^3	τ^3	τ^3	τ^3	τ^3	τ^3	(1,0,1)
#20	-1	$i\tau^3$	$i\tau^3$	τ^3	τ^1	0	τ^1	τ^1	τ^1	0	(0,0,1)

Table I: Summary of 20 distinct symmetric Z_2 spin liquids on triangular lattice. Among them, 8 states have their counterparts in the Schwinger-boson representation³¹. We use $[x, y] \equiv \langle 0, 0 | x, y \rangle$ to label representative mean-field amplitudes. Only 4 Abrikosov fermion states support a symmetric Z_2 spin liquid with up to next nearest neighbor (NNN) mean-field amplitudes, as highlighted by red color. Each symmetric Abrikosov-fermion state have a unique nematic descendant which breaks C_6 rotation but preserves mirror reflections σ and $R = \sigma(C_6)^3$. In addition to the 4 symmetric ansatz, another 4 states support a nematic Z_2 spin liquid with up to NNN amplitudes, as highlighted by blue color. In the mean-field amplitudes, τ^1 represents real pairing while τ^3 stands for real hopping. Up to NNN mean-field amplitudes, only 3 ansatz support a gapped nematic Z_2 spin liquids: they are #1, #6 and #20 states.

Mean-field amplitude $\hat{\alpha} \equiv [1, 1]$ between nearest neighbors (NNs) must have

$$\begin{aligned} g_{\mathbf{T}} \hat{\alpha} g_{\mathbf{T}}^{\dagger} &= -\hat{\alpha}, \\ \hat{\alpha} &= \eta_{12} g_{\sigma} \hat{\alpha} g_{\sigma}^{\dagger}, \\ \hat{\alpha}^{\dagger} &= \eta_{12} g_{C_6}^3 \hat{\alpha} g_{C_6}^{-3}. \end{aligned} \quad (10)$$

For next nearest neighbor (NNN) mean-field amplitude $\hat{\beta} \equiv [2, 1]$ we have

$$\begin{aligned} g_{\mathbf{T}} \hat{\beta} g_{\mathbf{T}}^{\dagger} &= -\hat{\beta}, \\ \eta_{12} g_{C_6} \hat{\beta} g_{C_6}^{\dagger} &= g_{\sigma} \hat{\beta} g_{\sigma}^{\dagger}, \\ \hat{\beta}^{\dagger} &= \eta_{12} g_{C_6}^3 \hat{\beta} g_{C_6}^{-3}. \end{aligned} \quad (11)$$

Among the 20 different Abrikosov fermion states summarized in TABLE I, only 4 states can realize a symmetric Z_2 spin liquid with up to NNN mean-field amplitudes. They are #1, #6, #18 and #20 as highlighted by red color in TABLE I. Later we'll show that #18 state doesn't support a gapped spinon spectrum with up to NNN amplitudes.

B. Duality between Abrikosov-fermion and Schwinger-boson representations

In Schwinger-boson representation³³, a spin-1/2 particle on lattice site \mathbf{r} is decomposed into two species of bosonic spinons $\{b_{\mathbf{r},\alpha} | \alpha = \uparrow / \downarrow\}$:

$$\vec{S}_{\mathbf{r}} = \frac{1}{2} \sum_{\alpha, \beta = \uparrow / \downarrow} b_{\mathbf{r},\alpha}^{\dagger} \vec{\sigma}_{\alpha, \beta} b_{\mathbf{r},\beta} \quad (12)$$

where $\vec{\sigma}$ are Pauli matrices. Similar to Abrikosov-fermion representation, the spin wavefunction is obtained by single-occupancy Gutzwiller projection on mean-field states of bosonic spinons. Schwinger-boson representation has a $U(1)$ gauge redundancy $b_{\mathbf{r},\sigma} \rightarrow e^{i\phi_{\mathbf{r}}} b_{\mathbf{r},\sigma}$ and hence any symmetry operation \hat{u} is followed by a $U(1)$ phase rotation of Schwinger bosons by angle $\phi_{\hat{u}}(x, y)$. Ref. 31 classified Z_2 spin liquids in Schwinger-boson representation and obtain 8 different states on triangular lattice, with the following gauge-inequivalent PSGs

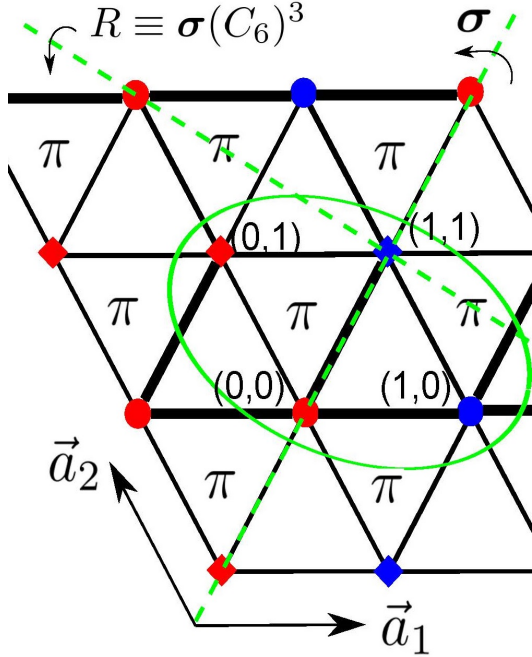


Figure 1: (color online) Crystal symmetry of triangular lattice, and nearest-neighbor (NN) hopping amplitudes of fermionic spinons in the π -flux state on the triangle lattice. All NN hoppings are real with the same magnitude $|\alpha| > 0$, where thick (thin) bonds have negative (positive) hopping signs. Each magnetic unit cell (denoted by the green oval) is chosen to contain 4 lattice sites labeled by red/blue diamonds/dots.

($p_i = 0, 1$):

$$\begin{aligned}\phi_{T_1}(x, y) &= 0, & \phi_{T_2}(x, y) &= xp_1\pi, \\ \phi_{\sigma}(x, y) &= (xy p_1 + p_2/2)\pi, \\ \phi_{C_6}(x, y) &= [p_1 y(x + \frac{y-1}{2}) + p_3/2]\pi.\end{aligned}\quad (13)$$

and one can always choose a gauge so that $\phi_{\mathbf{T}}(x, y) = 0$ for time reversal \mathbf{T} .

What is the relation between these 8 Schwinger-boson states and the 20 Abrikosov-fermion states obtained in this work? There are two ways to achieve this connection. The first approach is to directly compare the crystal symmetry (mirror reflection σ , R and inversion $(C_6)^3$) quantum numbers of their projected spin wavefunction on different finite lattices³⁴ and on infinite cylinders^{34,35}. For symmetry quantum numbers associated with time reversal symmetry (3 row at the bottom of TABLE II), one can compare the degeneracy in the entanglement spectra of their projected wavefunctions on different infinite cylinders with σ and R symmetries³⁴. Repeating the same analysis as in Ref. 34 we obtain the unification of Schwinger-boson PSGs and Abrikosov-fermion PSGs as shown in TABLE I.

Algebraic Identities	bosonic b_{σ}	fermionic f_{σ}	vison $v = b \times f$
$T_2^{-1}T_1^{-1}T_2T_1 = e$	$(-1)^{p_1}$	η_{12}	-1
$\sigma^{-1}T_1\sigma T_1^{-1} = e$	1	1	1
$\sigma^{-1}T_2\sigma T_2^{-1} = e$	1	1	1
$C_6^{-1}T_1C_6T_2 = e$	1	1	1
$C_6^{-1}T_2C_6T_2^{-1}T_1^{-1} = e$	1	1	1
$\sigma^2 = e$	$(-1)^{p_2}$	η_{σ}	1
$R^2 = (C_6\sigma)^2 = e$	$(-1)^{p_2+p_3}$	$\eta_{\sigma C_6}$	1
$(C_6)^6 = e$	$(-1)^{p_3}$	η_{C_6}	-1
$T_1^{-1}\mathbf{T}^{-1}T_1\mathbf{T} = e$	1	1	1
$T_2^{-1}\mathbf{T}^{-1}T_2\mathbf{T} = e$	1	1	1
$\sigma^{-1}\mathbf{T}^{-1}\sigma\mathbf{T} = e$	$(-1)^{p_2}$	$\eta_{\sigma\mathbf{T}}$	1
$R^{-1}\mathbf{T}^{-1}R\mathbf{T} = e$	$(-1)^{p_2+p_3}$	$\eta_{C_6\mathbf{T}\eta_{\sigma\mathbf{T}}}$	1
$\mathbf{T}^2 = e$	-1	-1	1

Table II: The correspondence between bosonic spinon³¹, fermionic spinon and vison PSGs on the triangular lattice. Here bosonic spinon (b_{σ}) PSGs are labeled by three integers³¹ $p_i = 0, 1$ ($i = 1, 2, 3$), while fermionic spinon (f_{σ}) PSGs are labeled by six integers ($\eta_{12}, \eta_{\sigma}, \eta_{\sigma C_6}, \eta_{C_6}, \eta_{\sigma\mathbf{T}}, \eta_{C_6\mathbf{T}}$) where $\eta = \pm 1$. Choosing a proper gauge we can always fix $C_6^{-1}T_2C_6T_2^{-1}T_1^{-1} = C_6^{-1}T_1C_6T_2 = 1$ for both spinons and visons.

The 2nd approach is to understand the vison PSGs in the Schwinger-boson state. As shown in³⁶ any Z_2 spin liquids constructed by projecting a mean-field Schwinger-boson state doesn't support gapless edge states. On the other hand, nontrivial vison PSGs, *e.g.* $\sigma^2 = -1$ or $\sigma\mathbf{T}\sigma^{-1}\mathbf{T}^{-1} = -1$ acting on visons v , will lead to symmetry protected gapless edge states on an open edge preserving reflection σ . These strong constraints can determine the vison PSGs in any Schwinger-boson state, as shown in the right column of TABLE II. Meanwhile, in a Z_2 spin liquid the fermionic spinon f_{σ} can be viewed as a bound state¹⁶ of a bosonic spinon b_{σ} and vison v due to fusion rule $f_{\sigma} = b_{\sigma} \times v$. Consequently the fermionic spinon (f) PSGs is a product of bosonic spinon (b) PSGs and vison (v) PSGs, multiplied by a twist factor^{21,34-36}. This twist factor is -1 in the case of $(C_6)^6 = e^{2\pi i}$, $\sigma^2 = R^2 = e^{3\pi i}$ and $\sigma\mathbf{T}\sigma^{-1}\mathbf{T}^{-1} = R\mathbf{T}R^{-1}\mathbf{T}^{-1} = e^{3\pi i}$, and +1 in all other cases.

As a result in TABLE II, a Schwinger-boson state (p_1, p_2, p_3) belong to the same symmetric Z_2 spin liquid phase as an Abrikosov-fermion state if their PSGs have the following correspondence:

$$\begin{aligned}\eta_{12} &= (-1)^{p_1}, \\ \eta_{\sigma} &= \eta_{\sigma\mathbf{T}} = \eta_{C_6}\eta_{\sigma C_6} = (-1)^{p_2+1}, \\ \eta_{C_6} &= \eta_{C_6\mathbf{T}} = (-1)^{p_3}.\end{aligned}\quad (14)$$

All 8 Schwinger-boson states have their counterparts in Abrikosov-fermion representation, as summarized in TABLE I. Since the continuous phase transitions between Z_2 spin liquids and noncollinear magnetic orders can be simply achieved by condensing bosonic spinons^{27,28} in

the Schwinger-boson representation, this unification allows us to understand the neighboring magnetic orders of some Abrikosov-fermion states.

C. Nematic descendants

DMRG studies^{12,13} suggest strong evidence for nematic order in the gapped spin liquid phases, *i.e.* spontaneously broken C_6 rotational symmetry coexisting with Z_2 topological order. This motivates us to study nematic (or anisotropic) Z_2 spin liquids on a triangular lattice. In spite of broken C_6 symmetry, these nematic Z_2 spin liquids still preserve two mirror reflections^{12,13}, σ and $R \equiv \sigma(C_6)^3$, as well as their combination: site-centered inversion symmetry $I = (C_6)^3$. Ref. 37 classified nematic Z_2 spin liquids on an anisotropic triangular lattice (with σ and R symmetry), leading to at least 63 distinct Abrikosov-fermion states. Instead of examining all these states, here we focus on those nematic states in proximity to a C_6 -symmetric Z_2 spin liquids. In other words they can be achieved by adding anisotropic perturbations to a C_6 -symmetric Z_2 spin liquid, *i.e.* one of the 20 states in TABLE I.

It turns out each of the 20 Abrikosov-fermion states summarized in TABLE I has a unique nematic descendant with the following symmetry transformations

$$\begin{aligned} G_{T_1}(x, y) &= 1, & G_{T_2}(x, y) &= \eta_{12}^x, \\ G_{\sigma}(x, y) &= \eta_{12}^{xy} g_{\sigma}, & G_I(x, y) &= \eta_{12}^{x+y} (g_{C_6})^3, \\ G_R(x, y) &= \eta_{12}^{xy+x+y} g_R, & G_{\mathbf{T}}(x, y) &= g_{\mathbf{T}} = i\tau^2. \end{aligned}$$

where $g_R \equiv g_{\sigma}(g_{C_6})^3$. These symmetry properties impose the following constraints on a generic mean-field amplitude $[x, y] \equiv \langle 0, 0 | x, y \rangle$:

$$g_{\mathbf{T}}[x, y] g_{\mathbf{T}}^{\dagger} = -[x, y], \quad (15)$$

$$g_{C_6}^3[x, y] g_{C_6}^{-3} = \eta_{12}^{xy+x+y} [x, y]^{\dagger}, \quad (16)$$

$$g_{\sigma}[x, x] g_{\sigma}^{\dagger} = \eta_{12}^x [x, x], \quad (17)$$

$$g_R[x, -x] g_R^{\dagger} = \eta_{12}^x [x, -x]. \quad (17)$$

To be specific, there are two independent amplitudes between 1st nearest neighbors (NNs) *i.e.* $[1, 0]$ and $[1, 1]$ in nematic states. They satisfy

$$\begin{aligned} g_{\mathbf{T}}[1, 0] g_{\mathbf{T}}^{\dagger} &= -[1, 0], \\ g_{C_6}^3[1, 0] g_{C_6}^{-3} &= \eta_{12}[1, 0]^{\dagger}. \end{aligned} \quad (18)$$

and

$$\begin{aligned} g_{\mathbf{T}}[1, 1] g_{\mathbf{T}}^{\dagger} &= -[1, 1], \\ g_{C_6}^3[1, 1] g_{C_6}^{-3} &= \eta_{12}[1, 1]^{\dagger}, \\ g_{\sigma}[1, 1] g_{\sigma}^{\dagger} &= \eta_{12}[1, 1]. \end{aligned} \quad (19)$$

Similarly, two independent 2nd NN amplitudes $[2, 1]$ and $[1, -1]$ satisfy

$$\begin{aligned} g_{\mathbf{T}}[2, 1] g_{\mathbf{T}}^{\dagger} &= -[2, 1], \\ g_{C_6}^3[2, 1] g_{C_6}^{-3} &= \eta_{12}[2, 1]^{\dagger}. \end{aligned} \quad (20)$$

and

$$\begin{aligned} g_{\mathbf{T}}[1, -1] g_{\mathbf{T}}^{\dagger} &= -[1, -1], \\ g_{C_6}^3[1, -1] g_{C_6}^{-3} &= \eta_{12}[1, -1]^{\dagger}, \\ g_{\sigma}[1, -1] g_{\sigma}^{\dagger} &= [1, -1]^{\dagger}. \end{aligned} \quad (21)$$

These conditions give rise to symmetry-allowed mean-field amplitudes for the 20 nematic Z_2 spin liquids, as summarized in TABLE I. Due to spontaneous breaking of C_6 rotational symmetry, the symmetry conditions for nematic Z_2 spin liquids are less stringent than for the isotropic (C_6 symmetric) ones, leading to nonzero NN and NNN amplitudes that are not allowed in isotropic states. As a consequence, 4 more states support a nematic Z_2 spin liquid with up to NNN mean-field amplitudes, in addition to the 4 isotropic states (red-colored in TABLE I) in isotropic case. They are #4, #7, #10 and #13, as highlighted by blue color in TABLE I.

III. GAPPED SYMMETRIC Z_2 SPIN LIQUIDS AND THEIR NEIGHBORING PHASES

In DMRG studies of spin-1/2 J_1 - J_2 Heisenberg model, the gapped spin liquid phase appear only in the parameter range^{12,13} of $J_2/J_1 \leq 0.17$. Therefore for candidate Z_2 spin liquids in Abrikosov-fermion representation, we focus on Z_2 spin liquid states that can be realized by up to next nearest neighbor (NNN) mean-field amplitudes. In particular we'll start from mean-field ansatz with nonzero nearest neighbor (NN) amplitudes. We can always choose a proper gauge such that NN mean-field amplitudes are all real hoppings (τ^3).

There are only two possible NN hopping ansatz that preserve all symmetries (time reversal, spin rotation and crystal symmetries):

(I) uniform RVB state: all NN real hoppings share the same amplitude α .

(II) π -flux (algebraic spin liquid) state: π flux is inserted in half of the triangles (see FIG. 1).

They correspond to two distinct symmetric $U(1)$ spin liquids on triangular lattice, which host gapless fermionic spinons coupled to $U(1)$ gauge field. In the following we'll study candidate Z_2 spin liquids by adding perturbations to these two parent $U(1)$ spin liquids.

A. Gapped Z_2 spin liquids near uniform RVB state

Among the 20 states in TABLE I, 4 of them support uniform NN real hoppings, corresponding to 4 symmetric Z_2 spin liquids in the neighborhood of uniform RVB

state. They are #1, #5, #13 and #19 states. Three of these 4 states (#5, #13 and #19) only allow real hoppings up to NNN amplitudes, therefore remaining to be gapless $U(1)$ spin liquids with spinon fermi surfaces.

On the other hand, #1 state allow uniform hoppings and pairings in NN and NNN amplitudes. It's straightforward to verify that uniform pairing terms can open up a gap on the spinon fermi surface of NN hoppings, giving rise to a gapped Z_2 spin liquid which preserves all symmetries. Therefore #1 state, which is dual to Schwinger-boson (1,1,0) state, is the only gapped Z_2 spin liquid phase in the neighborhood of uniform RVB state.

B. Gapped Z_2 spin liquids near π -flux algebraic spin liquid

Unlike the uniform RVB state with a spinon fermi surface, the π -flux state³⁸ is an algebraic spin liquid^{26,39}, described by gapless Dirac fermions coupled to emergent $U(1)$ gauge field. Similar to the case of uniform RVB state, there are 4 distinct Z_2 spin liquids in the neighborhood of π -flux state: *i.e.* #10, #12, #18 and #20 states in TABLE I.

Choosing the 4-site magnetic unit cell as illustrated in FIG. 1, the Bloch Hamiltonian in the basis of $\psi_{(r_1, r_2), \sigma} \equiv (f_{(2x, 2y+1), \sigma}, f_{(2x+1, 2y+1), \sigma}, f_{(2x, 2y), \sigma}, f_{(2x+1, 2y), \sigma})^T$ writes

$$\hat{H}_{MF}^\pi = \alpha \sum_{\mathbf{k}, \sigma} \psi_{\mathbf{k}, \sigma}^\dagger \hat{h}_{\mathbf{k}} \psi_{\mathbf{k}, \sigma}, \quad \hat{h}_{\mathbf{k}} = \begin{pmatrix} 0 & 1 + e^{-ik_1} & 1 + e^{ik_2} & e^{ik_2} - e^{-ik_1} \\ 1 + e^{ik_1} & 0 & e^{i(k_1+k_2)} - 1 & 1 + e^{ik_2} \\ 1 + e^{-ik_2} & e^{-i(k_1+k_2)} - 1 & 0 & -1 - e^{-ik_1} \\ e^{-ik_2} - e^{ik_1} & 1 + e^{-ik_2} & -1 - e^{ik_1} & 0 \end{pmatrix}$$

The dispersion crosses zero energy (fermi level) at momentum $k_1 = k_2 = \pi$. Expanding the above Bloch Hamiltonian around Dirac point (π, π) leads to the following linearized Dirac Hamiltonian in the basis of $\psi_{\mathbf{q}+(\pi, \pi), \sigma}$

$$\hat{h}_{\mathbf{k}} = [-q_1 \mu_z \nu_y + q_2 \mu_y \nu_0 + (q_1 + q_2) \mu_x \nu_y] \sigma_0 + O(|\mathbf{q}|^2) \\ = \sqrt{6}(q_x \gamma_x + q_y \gamma_y) + O(|\mathbf{q}|^2), \\ \gamma_x = \frac{(\mu_x - 2\mu_z) \nu_y - \mu_y \nu_0}{\sqrt{6}}, \quad \gamma_y = \frac{\mu_x \nu_y + \mu_y \nu_0}{\sqrt{2}}, \\ \mathbf{q} = \mathbf{k} - (\pi, \pi) \equiv (q_1, q_2) = (2q_x, \sqrt{3}q_y - q_x).$$

where $\vec{\nu}$ and $\vec{\mu}$ are Pauli matrices for the (diamond, dot) and (red, blue) sublattice indices respectively (see FIG. 1), while $\vec{\sigma}$ are Pauli matrices associated with spin index. We've set lattice constant as unity.

In the Nambu basis of $\Psi_{\mathbf{q}} \equiv (\psi_{\mathbf{q}, \sigma}^T, -i\psi_{-\mathbf{q}, \sigma}^\dagger \sigma_y)^T$, the low-energy Dirac Hamiltonian writes

$$\hat{H}_{Dirac}^\pi = \frac{\alpha}{2} \sum_{\mathbf{q}} \Psi_{\mathbf{q}}^\dagger \hat{d}_{\mathbf{q}} \Psi_{\mathbf{q}}, \quad (22)$$

$$\hat{d}_{\mathbf{q}} = [-q_1 \mu_z \nu_y + q_2 \mu_y \nu_0 + (q_1 + q_2) \mu_x \nu_y] \sigma_0 \tau_z \\ = \sqrt{6}[q_x \gamma_x + q_y \gamma_y] \sigma_0 \tau_z.$$

where $\vec{\tau}$ are Pauli matrices for Nambu index.

A gapped Z_2 spin liquid can be obtained by adding pairing terms, which open up a gap in the Dirac spectrum. These pairing ‘‘mass terms’’ for Dirac fermions, however, may break certain symmetries. In particular, Dirac fermion $\Psi_{\mathbf{q}} = \sigma_y \tau_y \Psi_{-\mathbf{q}}^*$ in (22) transform under symmetries in the following way:

$$\Psi_{\mathbf{q}} \xrightarrow{T} i\sigma_y \Psi_{-\mathbf{q}}, \\ \Psi_{\mathbf{q}} \xrightarrow{SU(2)_{spin}} \exp(i\frac{\theta}{2} \hat{n} \cdot \vec{\sigma}) \Psi_{\mathbf{q}}, \\ \Psi_{\mathbf{q}} \xrightarrow{T_1} \mu_0 \nu_y \sigma_0 \tau_z \Psi_{\mathbf{q}}, \\ \Psi_{\mathbf{q}} \xrightarrow{T_2} \mu_y \nu_z \sigma_0 \tau_z \Psi_{\mathbf{q}}, \\ \Psi_{(q_1, q_2)} \xrightarrow{\sigma} U_{\sigma} \sigma_0 (i\tau_y g_{\sigma}) \Psi_{(q_2, q_1)}, \\ \Psi_{(q_1, q_2)} \xrightarrow{R=\sigma C_6^3} U_R \sigma_0 (g_{\sigma} g_{C_6}^3) \Psi_{(-q_2, -q_1)}, \\ \Psi_{(q_1, q_2)} \xrightarrow{C_6} U_{C_6} \sigma_0 (i\tau_y g_{C_6}) \Psi_{(-q_2, q_1+q_2)}.$$

where we have $[g_{C_6}, \tau_z] = [g_{\sigma}, \tau_z] = 0$ and

$$U_{\sigma} = U_R = \begin{pmatrix} 0 & 0 & 0 & 1 \\ 0 & -1 & 0 & 0 \\ 0 & 0 & 1 & 0 \\ 1 & 0 & 0 & 0 \end{pmatrix}, \quad U_{C_6} = \begin{pmatrix} 0 & 0 & 0 & -1 \\ 1 & 0 & 0 & 0 \\ 0 & 0 & 1 & 0 \\ 0 & -1 & 0 & 0 \end{pmatrix}.$$

Notice that there is a $U(1)$ gauge redundancy for algebraic spin liquid (22), *i.e.* the Dirac Hamiltonian is invariant under any τ_z rotations.

Clearly the symmetric spin-singlet pairing mass terms which anticommute with Dirac matrices $\gamma_{x,y} \sigma_0 \tau_z$ are simply

$$\mathbf{M}_{sSC} = \mu_0 \nu_0 \sigma_0 (\Re \Delta_{ssc} \cdot \tau_x + \Im \Delta_{ssc} \cdot \tau_y). \quad (23)$$

Time-reversal-invariant real pairing mass $\mu_0 \nu_0 \sigma_0 \tau_x$ preserves σ and C_6 symmetries, if and only if $\{g_{C_6}, \tau_x\} = \{g_{\sigma}, \tau_x\} = 0$. Therefore among the 4 neighboring Z_2 spin liquids near π -flux state, only #20 state with $g_{\sigma} = g_{C_6} = i\tau_z$ allows a symmetric pairing mass for the Dirac fermion.

As a result, #20 state which is dual to Schwinger-boson (0,0,1) state is the only gapped Z_2 spin liquid in the neighborhood of the π -flux algebraic spin liquid.

C. Confined symmetry-breaking phases in proximity to gapped Z_2 spin liquids

A gapped Z_2 spin liquid can be driven into ‘‘confined’’ symmetry-breaking phases with no fractional excitations, by condensing their fractional excitations. For example, condensing spin-singlet vison excitations typically gives rise to a valence bond solid (VBS) phase, which breaks crystal symmetries but preserves global spin rotation and time reversal symmetries. On the other hand, condensing bosonic spinons (carrying spin-1/2 each) typically leads

to a noncolinear magnetic order which breaks time reversal as well as spin rotational symmetries. Therefore confined symmetry-breaking states in proximity to a Z_2 spin liquid reflect the symmetry quantum numbers of spinons and visons therein, and is an important characterization of the symmetry fractionalization in the Z_2 spin liquid. In the following we analyze the proximate ordered phases of the two promising Z_2 spin liquids, #1 and #20 as discussed above.

First we discuss #1 state in the neighborhood of uniform RVB state. As shown in section IIB, it describes the same Z_2 spin liquid phase as the (1,1,0) state in Schwinger-boson representation³¹. In the Schwinger-boson representation, the transition from Z_2 spin liquid to a magnetic ordered phase is simply described by condensation of Schwinger-bosons. As shown in Ref. 31, the consequent ordered phase in proximity to (1,1,0) state is a 4-sublattice noncolinear magnetic order:

$$S(\mathbf{r}) = \mathbf{n}_1(-1)^x + \mathbf{n}_2(-1)^y + \mathbf{n}_3(-1)^{x+y}.$$

It features a 2×2 magnetic unit cell.

On the other hand, the low-energy dynamics of spinless visons is described by a fully frustrated quantum Ising model on the dual honeycomb lattice^{30,40}, which is constrained by the vison PSGs in TABLE II. As shown in Ref. 30,40–42, the VBS phase achieved by condensing visons in the Z_2 spin liquid is featured by an enlarged $\sqrt{12} \times \sqrt{12}$ unit cell.

Now let's turn to #20 state in the neighborhood of π -flux algebraic spin liquid. It belongs to the same Z_2 spin liquid phase as (001) state in Schwinger-boson representation^{27,31}. Since all Z_2 spin liquids constructed from Schwinger-boson mean-field ansatz share the same vison PSGs³⁶, the VBS phase in proximity to #20 state generically has the same $\sqrt{12} \times \sqrt{12}$ symmetry-breaking pattern as the #1 state. Meanwhile upon condensation of bosonic spinons, Ref. 27,31 showed that the so-called 120-degree Neel ordered phase with a $\sqrt{3} \times \sqrt{3}$ magnetic unit cell will be developed from the (001) state.

Since #20 state can be obtained by adding a singlet pairing mass term to Dirac spinons in π -flux state, the Abrikosov-fermion representation provides an alternative way to understand the confined symmetry-breaking phases in its neighborhood. To be specific, the VBS phase corresponds to the following mass term added to Dirac spinons in (22):

$$\mathbf{M}_{VBS} = \vec{B} \cdot \mathbf{V} = \frac{1}{\sqrt{3}} \left[B_1(\mu_x + \mu_z - \mu_y \nu_y) + B_2(\nu_x + \mu_x \nu_z - \mu_z \nu_z) + B_3(\nu_z - \mu_x \nu_x + \mu_z \nu_x) \right] \tau_z \quad (24)$$

where we've only written down the Pauli matrices with a nonzero subscript. The VBS mass matrices \mathbf{V} are invariant under time reversal and spin rotations, but transform

nontrivially under space group symmetries:

$$\begin{aligned} T_1(V_1, V_2, V_3)T_1^{-1} &= (V_1, -V_2, -V_2), \\ T_2(V_1, V_2, V_3)T_2^{-1} &= (-V_1, -V_2, V_2), \\ \sigma(V_1, V_2, V_3)\sigma^{-1} &= (-V_3, V_2, -V_1), \\ C_6(V_1, V_2, V_3)C_6^{-1} &= (-V_2, V_3, -V_1). \end{aligned}$$

corresponding to crystal-symmetry-breaking VBS orders. It's straightforward to verify that 3 VBS masses $V_{1,2,3}$ anticommute with each other, and they all anticommute with the singlet pairing mass $\tau_{x,y}$ corresponding to Z_2 spin liquid phase. As a result the low-energy dynamics of 5-component mass-term vector

$$\vec{v} = (\Re\Delta_{ssc}, \Im\Delta_{ssc}, VBS_1, VBS_2, VBS_3)$$

is described by $O(5)$ non-linear sigma model (NLsM) with a Wess-Zumino-Witten (WZW) term^{43–45}. Such a WZW term can be derived by integrating out fermionic spinons in the Dirac Hamiltonian (22). It implies a continuous quantum phase transition^{36,46} between Z_2 spin liquid #20 ($\Delta_{ssc} \neq 0, VBS = 0$) and the VBS phase ($\Delta_{ssc} = 0, VBS \neq 0$).

Similarly the quantum spin Hall (QSH) mass terms to Dirac spinons

$$\mathbf{M}_{QSH} = \vec{n} \cdot \mathbf{m} = \frac{(\mu_x \nu_y + \mu_z \nu_y - \mu_y)(\vec{n} \cdot \vec{\sigma})\tau_z}{\sqrt{3}} \quad (25)$$

also anticommute with the singlet pairing masses. This indicates the dynamics of the following 5-component mass vector

$$\vec{v}' = (\Re\Delta_{ssc}, \Im\Delta_{ssc}, QSH_x, QSH_y, QSH_z)$$

is also captured by $O(5)$ NLsM with a WZW term. Once the Dirac spinons acquires a finite gap from the QSH mass term, the monopole of $U(1)$ gauge fields coupled to fermionic spinons will carry a spin quantum number due to QSH effect^{36,46,47}. Although QSH mass \mathbf{M}_{QSH} in (25) appear to preserve $U(1)$ spin rotation along \vec{n} -axis, the proliferation of monopole events in $U(1)$ gauge fluctuations will destroy the spin conservation along \hat{n} -axis, leading to a noncolinear magnetic order with 3 Goldstone modes^{36,46}. Therefore the WZW term for the quintuplet of singlet pairing and QSH masses implies a continuous quantum phase transition between 120-degree Neel order and Z_2 spin liquid #20, in accordance with Schwinger-boson (001) state^{27,31}.

In the phase diagram of triangular J_1 - J_2 Heisenberg model obtained in DMRG studies, the gapped spin liquid phase appear in proximity to 120-degree Neel order and another colinear "stripy" Neel order^{12,13}. This is another evidence in favor of #20 state (*i.e.* Schwinger-boson (0,0,1) state) as a promising candidate for the spin liquid found in J_1 - J_2 model.

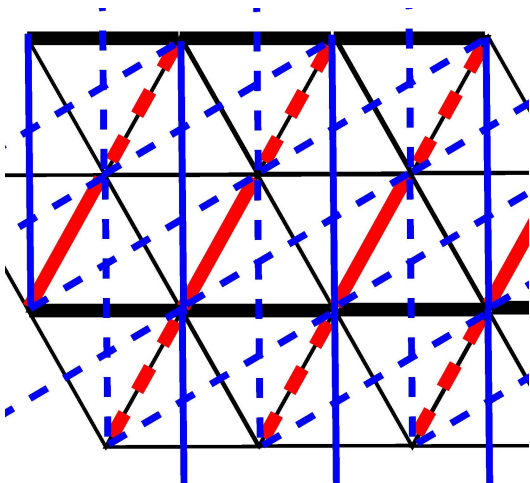


Figure 2: (color online) Mean-field hopping amplitudes (up to NNN) of nematic Z_2 spin liquid #20 in TABLE I. There are two types of NN hoppings denoted by black and red colors: for black ones, thick and thin lines have the same amplitude $|\alpha_1|$ but opposite signs; for red ones, solid and dashed lines have the same amplitude $|\alpha_2|$ but opposite signs. NNN amplitudes are labeled by blue color: solid and dashed lines have the same amplitude $|\beta_1|$ but opposite signs. Onsite real pairing is also allowed by symmetry.

IV. NEMATIC Z_2 SPIN LIQUIDS ON TRIANGULAR LATTICE

In DMRG studies of spin-1/2 J_1 - J_2 Heisenberg model on triangular lattice, both the even and odd sectors of the gapped spin liquid phase show spatially anisotropic spin-spin correlations^{12,13}, different from the Z_2 spin liquid in kagome Heisenberg model¹². Meanwhile the spin liquid shows strong response to a C_6 -breaking perturbation to Heisenberg couplings¹². This motivates us to seek for nematic Z_2 spin liquid candidates for J_1 - J_2 Heisenberg model. Again we focus on those nematic Z_2 spin liquids that can be realized by up to NNN mean-field amplitudes.

Nematic Z_2 spin liquids on triangular lattice has been classified in Ref. 37. Here we restrict ourselves to those nematic (anisotropic) Z_2 spin liquids that can be obtained by perturbing fully-symmetric (isotropic) Z_2 spin liquids. As discussed in section II C, for each symmetric Z_2 spin liquids on triangular lattice, there is one and only one nematic “descendant” which preserves two mirror reflections σ and R but breaks C_6 rotation (see FIG. 1). Their symmetry-allowed mean-field amplitudes are summarized in TABLE I.

First we examine those nematic Z_2 spin liquids in the neighborhood of uniform RVB state, #1, #5, #13 and #19. In addition to #1 state which already realizes a gapped Z_2 spin liquid without breaking C_6 symmetry, in the presence of nematic order #13 state can also realize a Z_2 spin liquid with up to NNN amplitudes. To be

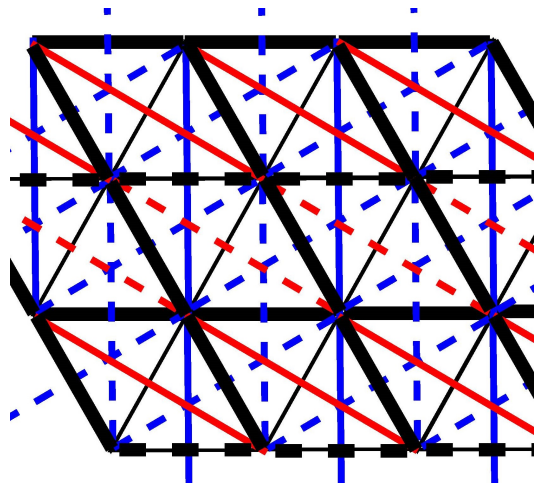


Figure 3: (color online) Mean-field hopping amplitudes (up to NNN) of nematic Z_2 spin liquid #6 in TABLE I. Nonzero NN hoppings are denoted by black thick lines: for black ones, solid and dashed lines have the same amplitude $|\alpha_1|$ but opposite signs. The thin lines connecting NNs have zero hopping amplitude. There are two types of NNN amplitudes: for blue (or red) colors, solid and dashed lines have the same amplitude $|\beta_1|$ (or $|\beta_2|$) but opposite signs. Onsite real pairing is also allowed by symmetry.

precise, C_6 symmetry breaking gives rise to nonzero pairing amplitudes (τ^1) in #13 state, as shown in TABLE I. However, these nematic pairing terms generally cannot open a full gap on the spinon fermi surface: typically they leave 4 point nodes on the fermi surface similar to the d-wave superconductors. Therefore even in the presence of nematic order, #1 state is still the only gapped Z_2 spin liquid near uniform RVB state.

Next we look into nematic Z_2 spin liquids in the neighborhood of π -flux state, #10, #12, #18 and #20. Among them, only ansatz #20 supports a fully-symmetric gapped Z_2 spin liquid. After breaking C_6 symmetry with nematic order, it is possible to realize a Z_2 spin liquid with up to NNN amplitudes in both #10 and #18 (but not #12) state. However, the pairing terms cannot open up a gap in the spinon Bogoliubov spectrum: point nodes still exist in #10 and #18 state. As a result, #20 is again the only gapped nematic Z_2 spin liquid near π -flux algebraic spin liquid. In addition to onsite real pairing, it also allows NN/NNN hoppings as demonstrated in FIG. 2.

Meanwhile, there are 3 other nematic Z_2 spin liquids that can be realized with up to NNN amplitudes: #4, #6 and #7. Among them, #4 and #7 have gapless excitations in their spinon Bogoliubov spectra, while #6 supports a gapped nematic Z_2 spin liquid. The mean-field ansatz #6 allows onsite real hoppings, together with NN/NNN real hoppings as demonstrated in FIG. 3.

To summarize, there are 3 gapped nematic Z_2 spin liquids that can be realized by up to NNN mean-field

amplitudes among the 20 states in TABLE I: they are #1 state dual to Schwinger-boson (110) state, #6 state, and #20 state dual to Schwinger-boson (001) state. They are the most promising candidate for possible nematic Z_2 spin liquid phase in triangular-lattice J_1 - J_2 Heisenberg model.

V. SUMMARY

To summarize, in this work we studied symmetry Z_2 spin liquids on triangular lattice and their nematic descendants, in connection to the numeric discovery of a gapped spin liquid phase in triangular lattice J_1 - J_2 model. We classified symmetric Z_2 spin liquids in the Abrikosov-fermion representation, found 20 distinct states and identified 2 states (#1 and #20 in TABLE I) as the promising candidates which support a gapped Z_2 spin liquid with up to NNN mean-field amplitudes. By establishing the correspondence between symmetric Abrikosov-fermion and Schwinger-boson states on triangular lattice, we are able to understand the noncollinear magnetic order phases and VBS phases in the neighborhood of these 2 gapped spin liquids. In particular state #20 in TABLE I, dual to the (001) state in Schwinger-boson representation, is continuously connected to the 120-degree Neel order, which is found

to lie in proximity to gapped spin liquid in the DMRG phase diagram^{12,13}. Motivated by numerical evidence of possible nematic order in this spin liquid phase^{12,13}, we also studied nematic Z_2 spin liquids by perturbing the symmetric ones. We identified 3 promising nematic states, #1, #6 and #20 in TABLE I which can realize a gapped Z_2 spin liquid with up to NNN amplitudes. It'll be interesting for future variational Monte Carlo studies to see whether these nematic Z_2 spin liquids are energetically more favorable than fully-symmetric states or not.

Note added: Upon completion of this paper, we became aware of an independent work⁴⁸ which also classified symmetric Z_2 spin liquids in the Abrikosov-fermion representation on triangular lattice.

Acknowledgments

I'm grateful to Zhenyue Zhu and Donna D. N. Sheng for helpful discussions, and especially to Biao Huang and Nandini Trivedi for collaborations on related topics. I thank the hospitality of Tao Li at Renmin University and the Aspen Center for Physics, where part of this work was finished. This work is supported by startup fund at Ohio State University and in part by NSF Grant No. PHYS-1066293 (YML).

-
- ¹ L. Balents, Nature **464**, 199 (2010), ISSN 0028-0836.
² P. A. Lee, Journal of Physics: Conference Series **529**, 012001 (2014), ISSN 1742-6596.
³ S. Yan, D. A. Huse, and S. R. White, Science **332**, 1173 (2011).
⁴ S. V. Isakov, M. B. Hastings, and R. G. Melko, Nat Phys **7**, 772 (2011), ISSN 1745-2473.
⁵ H.-C. Jiang, Z. Wang, and L. Balents, Nat Phys **8**, 902 (2012), ISSN 1745-2473.
⁶ S. Depenbrock, I. P. McCulloch, and U. Schollwöck, Phys. Rev. Lett. **109**, 067201 (2012).
⁷ H.-C. Jiang, H. Yao, and L. Balents, Phys. Rev. B **86**, 024424 (2012).
⁸ L. Wang, Z.-C. Gu, F. Verstraete, and X.-G. Wen, ArXiv e-prints 1112.3331 (2011).
⁹ B. Bauer, L. Cincio, B. Keller, M. Dolfi, G. Vidal, S. Trebst, and A. Ludwig, Nat Commun **5**, (2014).
¹⁰ S.-S. Gong, W. Zhu, and D. N. Sheng, Sci. Rep. **4**, (2014).
¹¹ Y.-C. He, D. Sheng, and Y. Chen, Phys. Rev. Lett. **112**, 137202 (2014).
¹² Z. Zhu and S. R. White, ArXiv e-prints (2015), 1502.04831.
¹³ W.-J. Hu, S.-S. Gong, W. Zhu, and D. N. Sheng, ArXiv e-prints (2015), 1504.00654.
¹⁴ S. A. Kivelson, D. S. Rokhsar, and J. P. Sethna, Phys. Rev. B **35**, 8865 (1987).
¹⁵ N. Read and B. Chakraborty, Phys. Rev. B **40**, 7133 (1989).
¹⁶ A. Y. Kitaev, Annals of Physics **303**, 2 (2003), ISSN 0003-4916.
¹⁷ M. Levin and X.-G. Wen, Phys. Rev. Lett. **96**, 110405 (2006).
¹⁸ A. Kitaev and J. Preskill, Phys. Rev. Lett. **96**, 110404 (2006).
¹⁹ R. V. Mishmash, J. R. Garrison, S. Bieri, and C. Xu, Phys. Rev. Lett. **111**, 157203 (2013).
²⁰ R. Kaneko, S. Morita, and M. Imada, J. Phys. Soc. Jpn. **83**, 093707 (2014), ISSN 0031-9015.
²¹ A. M. Essin and M. Hermele, Phys. Rev. B **87**, 104406 (2013).
²² A. Mesaros and Y. Ran, Phys. Rev. B **87**, 155115 (2013).
²³ H. Song and M. Hermele, Phys. Rev. B **91**, 014405 (2015).
²⁴ A. A. Abrikosov, Physics **2**, 5 (1965).
²⁵ I. Affleck, Z. Zou, T. Hsu, and P. W. Anderson, Phys. Rev. B **38**, 745 (1988).
²⁶ X.-G. Wen, Phys. Rev. B **65**, 165113 (2002).
²⁷ S. Sachdev, Phys. Rev. B **45**, 12377 (1992).
²⁸ A. V. Chubukov, S. Sachdev, and T. Senthil, Nuclear Physics B **426**, 601 (1994), ISSN 0550-3213.
²⁹ N. Read and S. Sachdev, Phys. Rev. Lett. **62**, 1694 (1989).
³⁰ R. Moessner and S. L. Sondhi, Phys. Rev. B **63**, 224401 (2001).
³¹ F. Wang and A. Vishwanath, Phys. Rev. B **74**, 174423 (2006).
³² G. Chen, A. Essin, and M. Hermele, Phys. Rev. B **85**,

- 094418 (2012).
- ³³ A. Auerbach, *Interacting electrons and quantum magnetism*, Graduate Texts in Contemporary Physics (Springer, New York, 1994).
- ³⁴ M. Zaletel, Y.-M. Lu, and A. Vishwanath, ArXiv e-prints (2015), 1501.01395.
- ³⁵ Y. Qi and L. Fu, Phys. Rev. B **91**, 100401 (2015).
- ³⁶ Y.-M. Lu, G. Y. Cho, and A. Vishwanath, ArXiv e-prints (2014), 1403.0575.
- ³⁷ Y. Zhou and X.-G. Wen, eprint arXiv:cond-mat/0210662 (2002), cond-mat/0210662.
- ³⁸ S. Rachel, M. Laubach, J. Reuther, and R. Thomale, Phys. Rev. Lett. **114**, 167201 (2015).
- ³⁹ M. Hermele, T. Senthil, and M. P. A. Fisher, Phys. Rev. B **72**, 104404 (2005).
- ⁴⁰ R. Moessner, S. L. Sondhi, and P. Chandra, Phys. Rev. Lett. **84**, 4457 (2000).
- ⁴¹ G. Misguich and F. Mila, Phys. Rev. B **77**, 134421 (2008).
- ⁴² K. Slagle and C. Xu, Phys. Rev. B **89**, 104418 (2014).
- ⁴³ A. G. Abanov and P. B. Wiegmann, Nuclear Physics B **570**, 685 (2000), ISSN 0550-3213.
- ⁴⁴ A. Tanaka and X. Hu, Phys. Rev. Lett. **95**, 036402 (2005).
- ⁴⁵ T. Senthil and M. P. A. Fisher, Phys. Rev. B **74**, 064405 (2006).
- ⁴⁶ Y.-M. Lu and Y. Ran, Phys. Rev. B **84**, 024420 (2011).
- ⁴⁷ Y. Ran, A. Vishwanath, and D.-H. Lee, arXiv:0806.2321v2 (2008).
- ⁴⁸ W. Zheng, J.-W. Mei, and Y. Qi, ArXiv e-prints (2015), 1505.05351.